Micron 150 (2021) 103138

Contents lists available at ScienceDirect

Micron

journal homepage: www.elsevier.com/locate/micron

Review

Traction force microscopy – Measuring the forces exerted by cells

Małgorzata Lekka *, Kajangi Gnanachandran, Andrzej Kubiak, Tomasz Zieliński, Joanna Zemła

Institute of Nuclear Physics, Polish Academy of Sciences, PL-31342, Cracow, Poland

ARTICLE INFO

Keywords:
Traction force microscopy
Cells
Traction in single cells and multicellular systems
2D/3D traction force microscopy

ABSTRACT

Cells generate mechanical forces (traction forces, TFs) while interacting with the extracellular matrix or neighbouring cells. Forces are generated by both cells and extracellular matrix (ECM) and transmitted within the cell-ECM or cell-cell contacts involving focal adhesions or adherens junctions. Within more than two decades, substantial progress has been achieved in techniques that measure TFs. One of the techniques is traction force microscopy (TFM). This review discusses the TFM and its advances in measuring TFs exerted by cells (single cells and multicellular systems) at cell-ECM and cell-cell junctional intracellular interfaces. The answers to how cells sense, adapt and respond to mechanical forces unravel their role in controlling and regulating cell behaviour in normal and pathological conditions.

1. Introduction

Over decades of research in mechanobiology had gathered much evidence showing that cells sense and adapt to the surrounding microenvironment both in normal and pathological conditions (Butcher et al., 2009; Janmey et al., 2009). Physical forces existing between the cell and extracellular matrix (ECM) or between cells participate, regulate, and govern various functional processes such as cell adhesion, migration, signalling, ion channel regulation, mechanotransduction (transmission of mechanical signal), and interaction between cells (Butcher et al., 2009; Janmey et al., 2009; Park et al., 2020; Wang, 2017). Apart from changes in cell morphology linked with the alteration of the cell mechanical properties (Lekka, 2016), the mechanical forces actively participate in the interaction of the cells with extracellular matrix components (Roca-Cusachs et al., 2017). These forces can be exogenous (generated outside of the cell, in the surrounding microenvironment) or endogenous (i.e., generated inside the cells). The latter are called traction forces (Hur et al., 2020). Traction forces (TFs) are defined as tangential tension exerted by cells either to the extracellular matrix (ECM) or the underlying substrate (Fig. 1A&B). Although TFs are generated inside the cell, they are transferred towards the cell microenvironment, regulating such phenomena as cell spreading and migration (Ladoux and Nicolas, 2012). They are transmitted through cell adhesive sites (i.e., focal adhesions, FAs). FAs serves as a link between ECM proteins and cell cytoskeleton, mainly actin filaments. On external (outside the cell), FAs involve such receptors as various integrins and proteoglycans (e.g., syndecans). On the internal part (inside the cell), they involve various proteins such as paxillin, vinculin, talin or actin (Case and Waterman, 2015). Therefore, the determination of TFs is useful not only in characterizing cell movement but also to help define phenotype changes in cells caused by biochemical and biomechanical treatments.

As numerous studies have demonstrated the TFs role in various biological processes, the need to quantify them arose in parallel. Various methods have been developed for measuring TFs in qualitative or quantitative ways. Although TFs visualization started from observing wrinkles formed on the thin elastic membrane by a single cell (Harris et al., 1980; Lee et al., 1994), the other approaches such as traction force microscopy (TFM) dominate nowadays (Butler et al., 2002; Hur et al., 2020; Style et al., 2014; Trepat et al., 2009). Over three decades of the TFM presence in research has produced many papers addressing various scientific problems resolved by this technique. Here, we briefly review the traction force microscopy principles and advances accompanied by the applications showing quantifications of traction forces in single cells and multicellular systems.

2. Traction force microscopy (TFM)

2.1. Principle of operation

Traction force microscopy measures the forces exerted by an adherent cell lying on a soft surface. The cell generates the TFs that deform it leading to the formation of a deformation field. The latter is used to calculate traction forces exerted at each contact point between a

* Corresponding author.
E-mail address: Malgorzata.Lekka@ifj.edu.pl (M. Lekka).

https://doi.org/10.1016/j.micron.2021.103138
Received 8 April 2021; Received in revised form 15 July 2021; Accepted 9 August 2021
Available online 12 August 2021

cell and substrate. Thus, intuitively, the principle of TFM is very straightforward, as presented in Fig. 1 C–H. Tiny fluorescently labelled beads are embedded in the substrate employed to trace induced by the cell deformation. Beads act as displacement markers and simultaneously facilitate the tracking of deformation and, indirectly, the displacement field calculations. Typically, bead positions are recorded with the cell attached to the surface and again after the cell detachment using, for example, trypsin (a serine protease that degrades cell adhesions). A comparison of these two images gives the displacements field. It should be underlined that TFs are not measured directly, but they are reconstructed from the deformations imposed by the cell to its surroundings (Roca-Cusachs et al., 2017). The underlying assumption is that the substrate mechanical properties are unchanged by the bead presence and that TFs acting perpendicularly to the substrate surface are negligible. Thus, an essential requirement for TFM is the ability to track the motion of the beads laterally.

When individual isolated cells are analyzed, local displacement is applied to calculate traction forces acting locally, regardless of 2D or 3D environments (Fig. 1A). In multicellular systems, global forces are derived, representing a force exerted by a cluster of cells, e.g. during collective migration (Fig. 1B). Although TFM is a relatively straightforward technique in its realization, it requires a mechanically adjustable substrate and optical system to detect bead displacement. The TFM simplicity does not translate directly into the interpretation of the results as the errors in TFs determination can be burden by several factors, including out-of-plane displacement data, resolution, noise, interpolation scheme, linear or nonlinear solutions, material nonlinearity, inaccurate determination of the cell contour, elastic inhomogeneities of the substrate or accuracy of the routines used to track bead positions.

2.2. Soft substrate used in TFM measurements

The substrates used in TFM are often thin films made of a flexible polymer, typically polyacrylamide (PA). PA forms a polymeric network of crosslinked acrylamide monomers. As a cross-linker a N,N'-methylene-*bis*-acrylamide (*bis*-acrylamide) is applied. The polymerization proceeds in the presence of ammonium persulfate and of N,N,N′,N′-tetramethyl ethylenediamine (TEMED). An alternative way of polyacrylamide poluymerization applied UV activatable irgacure (Sunyer et al., 2012). The change of the proportions of acrylamide and bis-acrylamide affects the porosity and mechanical properties of the prepared gels. Such PA functionality provides an easy means to reproduce deformable supports characterized by a large stiffness range (from single Pa to hundreds of kPa) that remains in the isotropic linear elastic regime. Stiffness can be

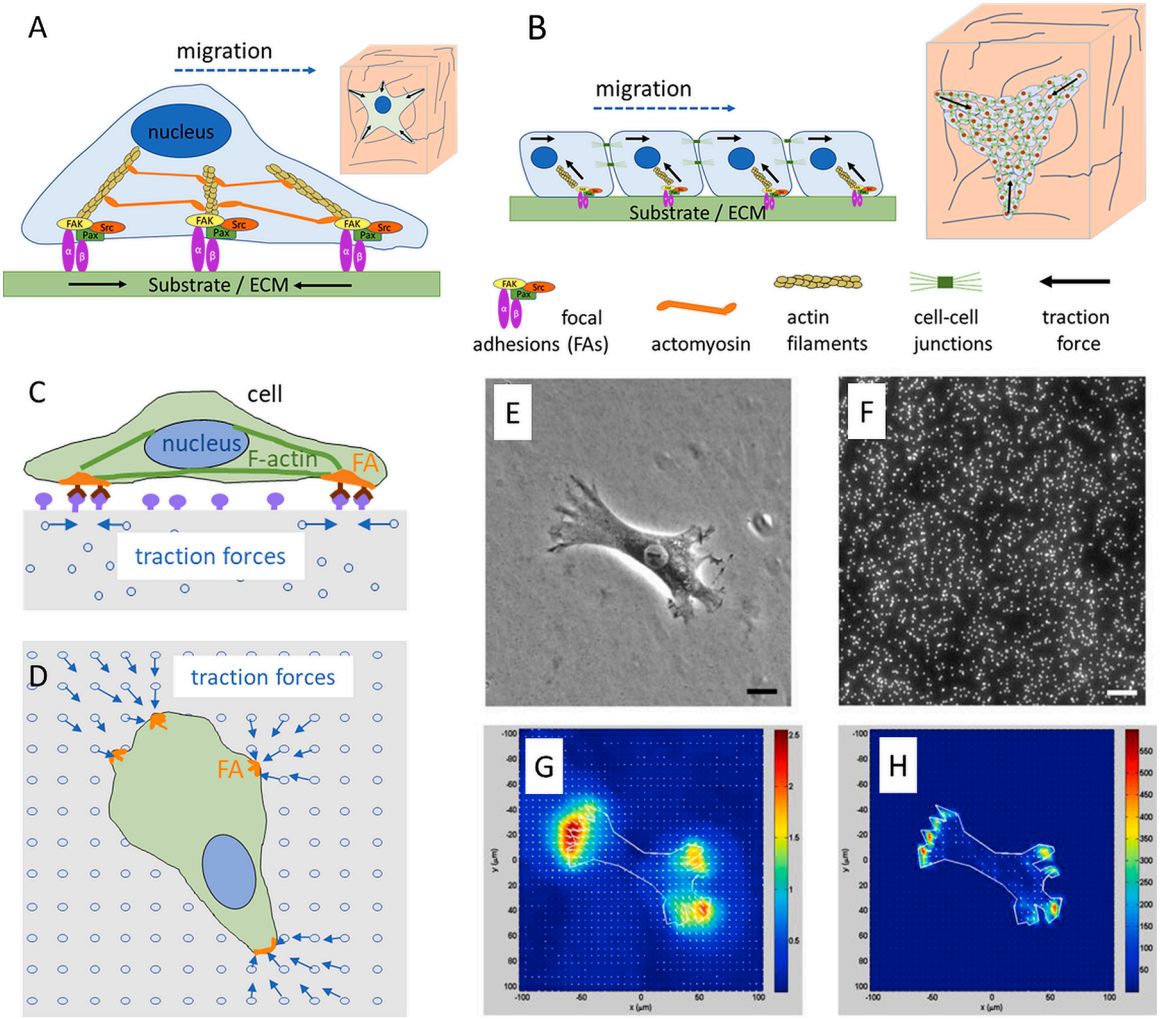

Fig. 1. (A&B) An illustration of traction forces in 2D (A) and 3D (B) environments for single cells and multicellular systems. C) The idea of traction force microscopy (TFM). A cell is cultured on an elastic substrate (typically polyacrylamide gel) with embedded fluorescent beads. The cell generates traction forces that deform it (D). Generated traction forces (arrows) within the focal adhesions (FA) are transmitted to integrins causing the bead displacement. An optical microscope records the displacement of the beads at the focal plane. The deformation is measured as a displacement of fluorescent beads embedded in the gel. Taking the bead images with (E) and without the cell (F), a displacement map can be calculated by comparing the positions of the beads (G*H) (E-F images were reprinted under creative commons license from Li et al. Sensors 10 (2010) 9948).

tuned correspondingly to physiologically relevant mechanics of ECM (Bachmann et al., 2020; Pelham and Wang, 1997).

Embedding beads in PA hydrogels results in the bead locations at various focal planes, contributing to a lower displacement accuracy. Instead of mixing hydrogels with fluorescent beads, several methods have been proposed to coat hydrogel surface with fluorescent beads using micro-contact (Schwarz et al., 2003) or nanodrip (Bergert et al., 2016). Such embedding increases the accuracy of the displacement acquisition. Also, the knowledge of the mechanical properties of a deformable surface is essential for calculating the force. Many distinct methods can be applied to characterize hydrogels mechanically, including atomic force microscope (AFM, (Zemła et al., 2020) or rheometer (Pogoda et al., 2017).

Living cells do not grow directly on a surface PA surface; thus, ECM proteins must be attached to PA surfaces by applying covalent cross-linking to provide favourable cell growth conditions. Typically, sulfo-succinimidyl 6-(4-azido-2-nitrophenylamino)hexanoate, so-called sulpho-SANPAH is applied as a covalent linker between proteins and PA surface (Kandow et al., 2007; Pelham and Wang, 1997). Sulfo-SANPAH is a heterobifunctional crosslinker with a phenylazide and a N-hydroxysuccinimide (NHS) ester group. Upon activation with light, the phenylazide group binds to any chemically stable molecule using a nonspecific covalent bond. The NHS ester group present on the other end of the crosslinker binds to the protein amines. Although sulpho-SANPAH is the most frequently used, another surface modification method can also be applied, employing such linkers as hydrazine hydrate (Damljanović et al., 2005; Tang et al., 2012). Such linkers can also be added to the PA precursor solutions and dispersed throughout the hydrogel. Many of them work similarly to sulpho-SANPAH as they form bonds to amines in the protein backbone. However, a concern of a lack of control of protein specificity still exists due to the nonspecific character of bonds, the protein orientation, their number, and the exposure of the binding sites are highly variable. The group of ECM proteins that could be attached to the PA surface is unlimited. Most of the experiments carried out for individual cells employed fibronectin, then collagen, laminin, and others. Balancing the stiffness of the hydrogel substrate is not easy due to the wide range of traction stress generated by cells. On one side, such surfaces have to provide a high signal-to-noise ratio (SRN) during acquiring cell images. On the other side, they have to be deformable enough to record bead displacements generated by cells. The magnitude of traction forces is cell-dependent. For example, T3T fibroblasts generate traction stress within the range of 0.25−0.5 kPa on PA surface within the range of 2.8–30 Pa (Oakes et al., 2014). Cancerous T24 cells (bladder cancer - transitional cell carcinoma) generate traction stress of 0.2 – 0.8 kPa on a 2–10 kPa PA surface.

Polyacrylamide is not the only hydrogel material applied in TFM. Other deformable hydrogels include collagen (Gjorevski and Nelson, 2012; Hall et al., 2013), gelatin (Doyle and Lee, 2002), hyaluronic acid (Mandal et al., 2019), and fibrin (Toyjanova et al., 2014b). These hydrogels have a more complex structure than PA, and, frequently, the linear elastic regime is narrow. Linear elasticity facilitates the calculation of traction forces. Gelatin gel seems to be alterative to PA as it possesses several similarities such as biocompatibility or easiness of its preparation. The stiffness (2–16 kPa as reported by Doyle and Lee, 2002) is controlled by gelatin concentration resulting in a narrower stiffness range than for PA. The stiffness of such gels varies between few tens to hundreds kPa. Collagen gels are more physiologically relevant as collagen fibres are present and formed during distinct normal and pathological processes occurring during cell life. Collagen fibres tend to remodel during the applied load force (Carey et al., 2011). Such behaviour can work as a drawback due to the time needed for imaging but, on the other side, can be used to track forces generated by cells by tracking fluorescently labelled collagen fibres. Analogously as collagen, hyaluronic acid (HA) is also naturally present in the cell environment. The stiffness of HA hydrogels ranges from 2 to 8 kPa what makes them suitable for the cultures of the stem (Burdick and Chung, 2009) and cancer (e.g. Hu7 – hepatocyte-derived carcinoma, (Mandal et al., 2019)) cells. Collagen and fibrin hydrogels are primarily applied to encapsulate cells forming a physiologically relevant 3D environment and track forces generated by embedded cells. Thus, the interactions between cells and ECM can be studied. In one exemplary experiment, fibroblasts embedded in the collagen matrix reveal that forces exerted by these cells on collagen fibres caused isometric tension under the applied deformation, while, by contrast, fibroblasts remained mechanically unloaded when the deformation was released (Grinnell, 2000). The way how fibroblasts mechanically interact with collagen fibres affects the mechanisms regulating the wound healing related processes.

2.3. Methods of data analysis

In classical TFM, a comparison between images taken for fluorescent beads embedded in the soft substrate with and without cells delivers the displacement field used to compute the traction force field. An image comparison applies the digital image correlation methods such as particle tracking/image velocimetry (PTV/PIV (Butler et al., 2002)) or correlation-based PTV (Butler et al., 2002) or feature-based registration (Yang et al., 2006). Several approaches have been proposed starting from the analytical one relying on the Boussinesq solution (either with Bayesian (Dembo and Wang, 1999; Schwarz et al., 2002) or Fourier transform (Butler et al., 2002; Yang et al., 2006) based calculations) or on effective pattern recognition combined with finite element method (FEM (Yang et al., 2006)).

Boussinesq approach describes the displacement of the bead in the surface of an infinite homogenous linear elastic half-space. The displacements originate from an applied point-load. The displacement vectors at the load points are assumed to result from the combined influence of a set of discrete point force vectors located at another set of points. The Boussinesq solution for a single force relates the displacement and force vectors within the half-space with specific the elastic (Young's) modulus. The primary assumption of the theoretical model is that cells are cultured on the infinite half-space. Hydrogel substrates have finite volume and thickness; therefore, they must be thick enough to fulfil the assumption. The considerations of the point surface load on the gel surface have shown that using Boussinesq solution for infinite half-space approximation generates errors in beads displacements depending on the gel thickness (Yang et al., 2006). The error increases with the larger distance from the point load. For example, traction forces burden by 10 % error when measured at the distance of 10 μm from the point load in on the 70 μm thick gel substrate. Increasing the gel thickness to 200 μm decreases the error below 5%. Typically, it is well-accepted that the gel thickness should be above 100 μm.

To enhanced TFM accuracy, a combination of pattern recognition with FEM was proposed in 2006 (Yang et al., 2006). In this approach, the beads are localized within the images of the PA substrate. The corresponding bead positions with and without TFs are then paired and used to derive the displacement field. Last, traction forces are computed using FEM. A pairing of beads involves the pattern recognition approach. Then, for each bead recorded in the image without TFs, the closest neighbours are found in the image with generated TFs. Both beads are connected. After finding all possible pairs from both images and finding the closest one, the displacement field is obtained. As the identified beads are randomly scattered over an image, a linear interpolation of the displacement field is applied to provide displacement in the FEM nodes. If the finite-element mesh is small enough and comparable with pixel size, FEM reproduces the substrate deformation caused by cellular traction force relatively well. Thus, FEM-derived force fields closely mimic the movement of beads (Holenstein et al., 2017). The displacements are calculated with high accuracy what translates into the reliable determination of traction forces generated by multiple cells.

Current TFs calculation methods involve several computational approaches. There are: solving boundary elements from displacement field using Bayesian statistics applied to solve the Boussinesq problem

(Dembo and Wang, 1999), using of Fourier transform to solve the Boussinesq equation (Butler et al., 2002), calculating of TFs for each FA separately assuming that TFs appear only within its area (Schwarz et al., 2002), and applying FEM (Yang et al., 2006).

3. Applications of TFM in biological research

3.1. Traction forces of single cells

The idea of traction forces originated in 1980 when thin polymeric silicone was applied as a substrate for cell culture (Harris et al., 1980). Migrating cells locally wrinkle the substrate indicating the presence of forces generated by a cell. TFs are generated by actomyosin interaction and actin polymerization, and intracellular proteins regulate them (Svitkina, 2018). TFs can be generated by single cells (Messi et al., 2020), clusters of cells (Tang et al., 2014) and even tissues (Pasqualini et al., 2018).

Traction force microscopy has initially been developed to measure TFs generated by single and isolated cells. Studies on cell migration and locomotion are probably the most typical TFM applications. During cell movement, actomyosin motors being central contractile machinery inside the cell, generate TFs that are further transmitted to ECM. Actomyosin is inherently contractile, in which myosin (specifically, myosin II) pulls on actin filaments. It induces the formation of fibres enabling cell motility (Fournier et al., 2010; Oliver et al., 1995; Wang and Lin, 2007; Wang and Wolynes, 2012). TFs are often polarised according to the direction of motion (Le Clainche and Carlier, 2008). Their magnitude and spatial distribution vary widely with the cell types. As TFs are transmitted to ECM through FAs, intuitively, they also affect cell morphology and adhesion. Indeed, over two decades of research has brought evidence that cells adjust their adhesive properties and morphology through the interaction with the surrounding microenvironment using TFs. FAs are composed of structural and signalling proteins, which physically link the actin cytoskeleton with the ECM (Roca-Cusachs et al., 2017). They provide a tool for two-ways transmitting routs for biochemical/biological to biomechanical or biomechanical into biochemical/biological signals. Starting from the molecular level, one of the most significant examples in which TFM was applied resolves the role of mechanical force in an actin-talin-integrin-fibronectin clutch (Elosegui-Artola et al., 2016). Transduction is triggered by talin unfolding after a specific threshold value of the traction force generated during the interaction of cells with ECM through FAs. In such conditions, talin unfolds and binds to vinculin, leading to increased adhesion and translocation of nuclear YAP (yes-associated protein, (Elosegui-Artola et al., 2016). The latter strongly evidences that TFs can modulate DNA synthesis (Wang et al., 2000), ECM protein secretion (Mark et al., 2020), or even gene expression (Medina et al., 2019). Other TFM studies increased our understanding of the TFs contribution in intra- and inter-cellular structures and their role in such processes as morphogenesis (Murray and Oster, 1984; Szabó and Mayor, 2015) and extracellular matrix behaviour (Ariyasinghe et al., 2017). By measuring the traction forces at the interface between cell–ECM, TFM significantly broadens our knowledge on mechanobiological parameters contributing to control and regulation of biomechanical response and cellular mechanotransduction (Del Álamo et al., 2007; Dembo and Wang, 1999; Polacheck and Chen, 2016; Razafiarison et al., 2018; Vining and Mooney, 2017). Several examples recalled here present TFs applicability of monitoring or related changes to specific diseases (Ariyasinghe et al., 2017; Floor et al., 2012; Li et al., 2017; McKenzie et al., 2018; Pasqualini et al., 2018; Peschetola et al., 2013; Wheelwright et al., 2018).

Cell motility plays an essential role in various biological processes, including the migration of cells in various diseases like cancer (Kai et al., 2016; Scotton et al., 2001). Intuitively, large TFs are generated by cardiac cells. Indeed, regardless of the conditions (normal or pathological), cardiac tissue has been shown to sense and respond to mechanical properties of the surrounding microenvironment (Ariyasinghe et al., 2017). In such a case, the quantitative TFs assessments can be applied to the contractile function marker (McCain et al., 2014). It is an attractive quantitative biomarker due to the potential applications of pluripotent stem cells in therapeutic interventions. Some studies focus on human-induced pluripotent stem cells (iPSCs) as they may become a potential source of spontaneously contracting cardiac myocytes. To successfully implement iPSCs-derived cardiomyocytes (iPSC-CMs), a significant level of traction forces should be achieved (Laflamme et al., 2007). TFM may track iPSC-derived cardiomyocyte maturation in conditions of variable calcium concentrations (Wheelwright et al., 2018). The obtained results have shown that iPSC-CMs cultured for two weeks generate smaller forces than cells cultured from one to three months. More extended iPSC-CMs cultures in conditions of physiologic calcium concentrations result in larger cells and more significant forces. The relation between cell morphology, substrate stiffness and forces showed a correlation between cell area and forces. Moreover, the TFs level can be linked with the energy production by primary cardiomyocytes (Pasqualini et al., 2018).

Cancer development and progression leads to cellular changes in many aspects, including cell biomechanics and adhesion (Floor et al., 2012). These two features are closely related to traction forces. Thus, if the biomechanical properties alter during oncogenic transformations (Lekka, 2016), intuitively, TFs alters too. Indeed, TFs generated by cancer cells are different as it has been reported for various cancer such as the bladder (Peschetola et al., 2013), breast (Li et al., 2017) or ovarian (McKenzie et al., 2018). Cell migratory properties of cancer cells are fundamental for preventing metastasis. Thus, knowing TFs may serve as an indicator of migration level. TFM experiments have delivered various results showing that TFs generation of the cancer-specific phenomenon. By comparing two bladder cancer cell lines, i.e. T24 cells being more invasive with RT112 (less invasive), it was possible to conclude that more invasive cells generate smaller TFs needed for migration. T24 cells were characterized by a well-differentiated actin cytoskeleton with large FAs. Less invasive RT112 cells exert larger TFs explained by larger (thicker) actomyosin cortex despite the formation of smaller focal adhesions (Peschetola et al., 2013). Oppositely, in breast cancer, the traction forces exerted by breast cancer cells (MCF7) are larger than the traction forces generated by non-tumorigenic breast epithelial cells (MCF 10A). A similar effect was observed for ovarian cancer cells seeded on stiffer substrates. Cells generated higher traction forces followed by enhanced migratory properties (McKenzie et al., 2018). Consequently, these cells exhibited durotaxis – the tendency to migrate in the gradient of stiffness in the most rigid substrate direction (Sunyer et al., 2016). These findings strongly link the traction forces and actin filaments with the poorly organized actin cortex in RT112 bladder cells.

Observed changes in TFs related to pathological conditions turn TFM towards monitoring the effect of anti-tumour drug action. For example, the use of α-difluoromethyl ornithine (DFMO, an anti-tumour drug indirectly targeting the actin filaments organization) decreases the magnitude of traction forces showing the potential applicability to monitor alterations in cell proliferation and migration in the presence of anti-tumour drugs (Li et al., 2017). In another study, the traction forces increased upon nocodazole treatment, leading to microtubule depolymerization (Rape et al., 2011). Two distinct mechanisms were found explaining the TFs origin. The first involved the activation of myosin II and is independent of tyrosine phosphorylation, while the other generates TFs independently of myosin II activity and is regulated by focal adhesion kinase (FAK). In both cases, TFs involved a microtubular network (Rape et al., 2011).

Knowing precisely how traction forces are generated enables finding the differences in the mechanics of the cell migration that could be used as a simple indicator of the stages of the cell motility cycle (Del Álamo et al., 2007). The TFs significance has been demonstrated for various cell types and distinct normal and disease-related processes.

3.2. Traction forces in multicellular systems

Studying traction forces generated by single isolated cells, although valuable, contradicts most physiological conditions in which cells interact with other cells. Thus, there was a need to quantify traction forces, at least for cell clusters not mentioned more complex multicellular systems such spheroids or tissues.

Cells communicate through the coupled biochemical and mechanical signalling pathways, regardless of the neighbouring cell type (Orzechowska et al., 2018; Reinhart-King et al., 2008; Tang et al., 2011, 2010). This interaction is not free from the presence of traction forces. When cells create a continuous monolayer within which each cell adheres to its neighbours and the underlying support, they migrate differently as a single cell. A single cell extends lamellipodia at its edge, being in contact with a substrate that induces polarized traction forces (Beningo et al., 2001). In the collective motion, a different mechanism has been observed (Trepat et al., 2009). In the case of the Madin-Darby Canine Kidney (MDCK) cells seeded on soft collagen-coated polyacrylamide gel (Young's modulus of 1.3 kPa), TFM revealed that the leader cell role is limited to local guidance. The traction forces generated by it are too small to guide a whole edge during collective migration. In collective migration, the traction forces are distributed throughout the whole migrating of the cell sheet, which is not guided by leader cells present at the monolayer edge (Trepat et al., 2009). Consequently, such cells can exhibit durotaxis, i.e., the tendency to migrate in the gradient of stiffness in the most rigid substrate direction (Sunyer et al., 2016). Durotaxis has already been shown to be more efficient for multicellular clusters than single cells due to the supracellular transmission of forces generated by cells migrating inside clusters (Sunyer et al., 2016).

In further studies, traction forces were generated during the cell pulling on the neighbouring cells (Liu et al., 2010; Maruthamuthu et al., 2011). It has already been reported that human pulmonary artery endothelial cells (HPAECs) generate cell-cell traction forces increasing with the cell-cell junction size (Liu et al., 2010). In MDCK cells, cell-cell traction forces were larger, but no correlation with the cell-cell junction size was found (Maruthamuthu et al., 2011). One of the TFM research directions applied to multicellular systems focuses on the forces between cells transmitted through adherens junctions involving cadherins (Mertz et al., 2013). The research has revealed that intercellular adhesions modulate forces transmitted to the ECM. Cadherin functions genetically silenced or inhibited using monoclonal antibody gather evidence showing that cadherin-based adhesion is essential for mechanical cooperativity of cells (Mertz et al., 2013). These findings underline the role of the cadherins in generating traction forces in such processes as cell development, homeostasis, and distinct pathologies. Moreover, when multicellular systems are considered, traction forces between cell-ECM and cell-cell contacts have to be considered to lead to the crosstalk phenomenon. Impairing the cell-ECM interaction might strengthen the cell-cell contacts. The importance of cell-ECM and cell-cell contacts is demonstrated in a study in which the microenvironment mimicking fibrosis of cardiac tissue has been engineered. In such pathological conditions, a link between cytoskeleton and force generation was small, suggesting that the cooperative balance between cell-matrix and cell-cell adhesions in the heart is guided by an architectural and functional hierarchy disrupted during disease progression (McCain et al., 2012). It seems that traction forces reorganizing the cell–ECM contacts are essential elements of the mechanism by which cadherin-based adhesion drive tissue morphogenesis and homeostasis.

Analogously as for TFs calculated for single cells, changes in TFs can be related to pathological conditions. For example, mutations in genes coding keratin are associated with diseases characterized by skin blistering observed in epidermolysis bullosa simplex (EBS, (Coulombe and Lee, 2012)). Keratins form keratin-based intermediate filaments. Mutation in keratin 14 leads to keratin aggregation and altered adhesion (Homberg and Magin, 2014). The research focused on keratin involvement in mechanotransduction within basal epidermis demonstrated that cells expressing keratins generate lower traction forces than keratin-deficient cells, that is accompanied by immature focal adhesions. The findings show that keratin filaments regulate mechanotransduction through a Rho signalling pathway. Moreover, keratin aggregates reduce directionality during collective migration, which guides the hypothesis that keratin networks contribute to traction force generation through actin reorganization and FA formation. Defects in force sensing and mechanotransduction associated with keratin mutations can contribute to EBS (Fujiwara et al., 2020).

Computing TFs for cell clusters is more complicated than the cell collective migration but simultaneously addresses various questions related to cell mechanics in the formation of spheroids or organoids, the dynamics and kinetics of such process, tissue network formation, or the interplay between paracrine and no-paracrine pathways of cellular signalling. An exemplary study has presented a robust finite-element based TFM to calculate traction forces produced by cell clusters consisting of multiple cells (Tang et al., 2014). The method accounted for the finite thickness of the substrate. Two main assumptions have been made. First, the cell cluster size can be larger than substrate thickness, and the other is that displacements data outside the cell cluster boundary can be neglected. These methods can be applied to compute traction forces for individual cell clusters of distinct size alone and close to each other. The experimental part was conducted for cell clusters composed of two types of cells, monkey kidney fibroblasts (MFK) and human colon cancer cells (HCT-8). The calculation of traction forces demonstrated that cell clusters behave as a single contractile unit in which the cells present in the outer layer serve as site needed to anchor the cluster in the underlying substrate. In such a case, the force is transmitted by cells located inside the cluster using probably cell-cell junctions and cytoskeleton. It was concluded that these cells are subjected to tensile intercellular forces as if the peripheral cells are pulling the interior cells outward. Traction is limited to small regions within the clusters. These regions can have locally balanced traction leaving the rest of the clusters nearly traction free and weakly adhered to the substrate.

In cell clusters (Fig. 2A&B) , traction forces are produced in specific domains placed inside the clusters. The domains alter dynamically upon various processes, like during the reported fusion of two clusters (Fig. 2C&D). The net force increased by about 20 folds, but the net force direction did not change compared to individual clusters with those in fusion (Tang et al., 2014). The fusion can be considered to merge two liquid droplets (Grosser et al., 2021). Thus, the location of traction domains can be linked with the minimization of surface energy.

Traction force determined for multicellular systems derived an average value of the force generated by a group of cells. A more heterogeneous population of cells, a wider the force distribution is, as each cell generate TFs in various range. The advantage is that the measured TFs are more physiologically relevant as *in vivo* conditions, cells interact among themselves. Gathered results support the applicability of TFM in tracing changes of multicellular systems. However, multicellular systems are inherently more complicated than single-cell systems because of intercellular adhesion and downstream signalling.

3.3. 3D traction force microscopy

Cells differently behave when cultured in the 3D matrix as they are supported from each side what changes their adhesive and migratory properties (Chang et al., 2013; Fraley et al., 2010; Meyer et al., 2012). Thus, it is reasonable to assume that TFs act in all directions. It was a driving force for further advancements in TFM is giving rise to 3D TFM. One of the earliest examples reported that cells seeded on 2D soft substrates exert 3D TFs. The study showed upwards and downwards TFs acting on the cell edge and nuclear region, respectively (Hur et al., 2009). Such a method enabled cell interaction in more physiologically relevant conditions to observe how different cellular regions contribute to cell migration or spreading. PA hydrogels are linear elastic materials, while most collagen-based not. As demonstrated by 3D viscoelastic TFM,

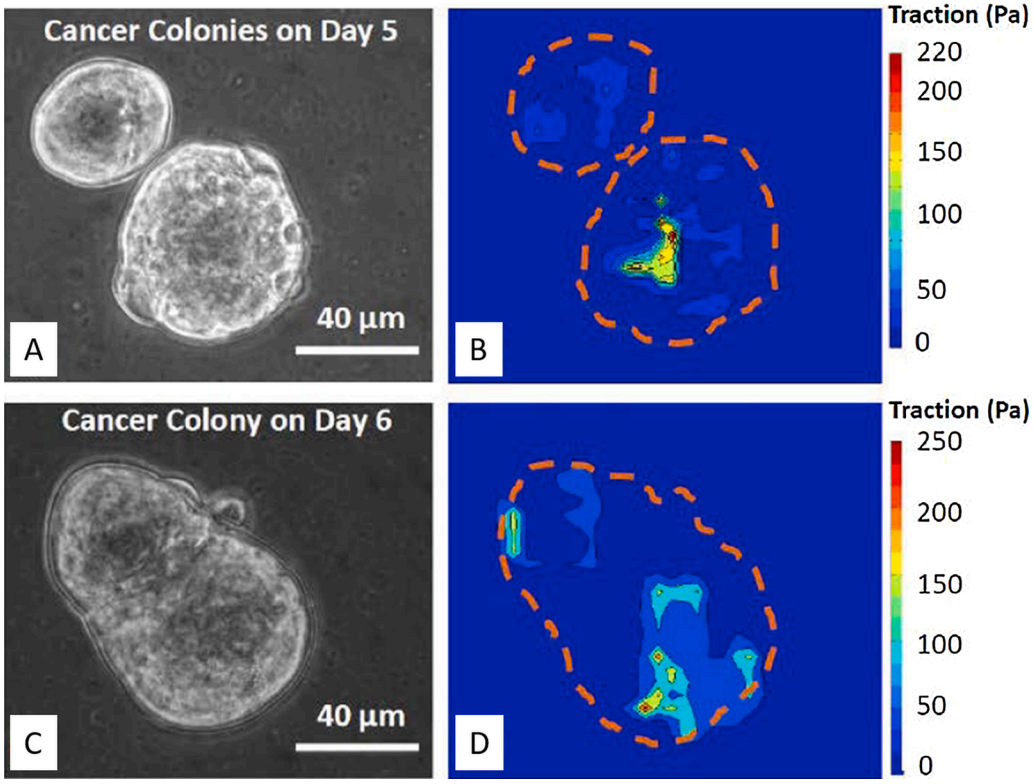

Fig. 2. Traction maps of human colon cancer cell (HCT-8) clusters. (A&B) phase-contrast image and traction stress map of two independent cancer cell clusters cultured on 2 kPa flexible hydrogel for 5 days. Each cluster generated high traction well inside the cluster, leaving its periphery almost traction-free. (C&D): phase-contrast image, and traction stress map during the fusion of HCT-8 cancer cell clusters after 24 h (6th culture day). **Reprinted under creative commons license from Tang et al. PLoS Comput Biol 10(6) (2014) e1003631).**

tractions forces can be obtained for cells cultured on materials with time-dependent nonlinear or viscous properties such as agarose gels (Toyjanova et al., 2014a). By applying various experimental and computational methods, the spatial distribution and magnitude of the time-dependent traction fields induced by viscoelastic substrate were obtained for breast cancer cells deforming collagen-functionalized agarose substrates.

More demanding approaches ask for quantification of TFs for cells embedded in a 3D soft microenvironment. Thus, further advancements in 3D TFM focuses on TFs generated by cells in 3D matrices providing a tool to measure the magnitude and 3D orientation of traction forces (Brockman et al., 2018; Legant et al., 2010). The 3D traction force microscopy idea is the same as for 2D TFM, i.e., recording fluorescent bead positions when the TFs are generated by cells and when TFs are released and calculating the 3D traction field. In an exemplary study, breast cancer cells (MDA-MB-231 cells) were embedded within the collagen I gel (Hall et al., 2013). The collagen-based hydrogels are generally not isotropic and purely linearly elastic. They also offer a space for cells to crawl deep into the gel confounding traction determination. Bead positions were acquired before and after TFs release. However, as it is challenging to remove cells from 3D hydrogel preserving its structure, the cytochalasin D treatment can be applied. Cytochalasin D disrupts actin filaments what leads to the TFs releasing. The obtained beads displacements served as a basis for the displacement field obtained for a 3D matrix volume surrounding individual cells. Preparing 3D hydrogels suitable to sense TFs is not the only obstacle as 3D TFM suffers from all limitations as 2D TFM. Despite that, measuring TFs from all directions introduced a tool for quantifying cell behaviour in native conditions. In the first reports, GFP-expressing fibroblasts were encapsulated in PEG (polyethylene glycol) hydrogels with an incorporated RGD sequence to which cells bind. Calculated TFs suggested that cells in 3D conditions probe ECM through strong inward tractions near the end of long, slender extensions (Legant et al., 2010). PEG hydrogels advantage is their linear elasticity, the more physiologically relevant hydrogels have been developed, such as collagen-based gels. It started from collagen gels populated with cells (Delvoye et al., 1991). A strain gauge generating electrical signal upon tension was recorded for cells embedded in the collagen network in this study. The results showed that fibroblast mechanical activity affects the structural organization of the dermis layer of healthy skin. In this study, the traction-related electric signal was shown to be dependent on a few factors such as cell type, their number and density, cytoskeleton organization, collagen concentration, and the amount of serum in the culture medium. TFs calculated for breast cancer cells (MDA-MB-231) reveal that these cells generate them at an almost constant level regardless of the collagen concentration related to matrix stiffness (Steinwachs et al., 2016). The results demonstrated that MDA-MB-231 cells glide through the gel continuously adhere to and de-adhere from collagen. In similar research, breast cancer cells were shown to induce collagen fibres alignment leading to local ECM stiffening. Generated larger TFs promote long-range displacement of cancer cells (Hall et al., 2016).

Altogether, these studies demonstrate a considerable potential of 3D TFM to probe traction forces generated by cells in a multidimensional environment of even viscoelastic nature. The gathered information will help unravel the mechanisms governing TFs transmission and transduction involving FAs, actin filaments and ECM remodelling.

3.4. *Advances beyond classical 2D traction force microscopy*

Although TFM has provided a deeper understanding of the role of physical forces during cellular homeostasis, disease progression, and many other cellular processes, still there is a need for improvements in the detection and quantification of traction forces. They encompass the experimental part by improving beads insertion into hydrogels, recording optical (fluorescent) images, and data analysis. Depending on the protocol of implementation, various spatial resolutions can be achieved. It varies from 0.4 µm to 7 µm for TFM measurements, in which substrate deformation is recorded. Using quantum dots provides 30−45 nm spatial resolution (Legant et al., 2013). A promising approach in the determination of traction forces is fluorescent detection linked with molecules genetically

expressed inside cells (Grashoff et al., 2010; Meng et al., 2008). Then, TFs were identified using molecules that could be immobilized on surfaces that enable targeting specific receptors on the cell membrane (Morimatsu et al., 2013). These molecules (called force tension sensors, FTSs) emit or alter fluorescence under tension produced by traction forces. FTSs provide high spatial and temporal resolutions and sensitivity (Polacheck and Chen, 2016). Furthermore, DNA or DNA-like materials has been applied to form the FTS constructs (Glazier et al., 2019). A summary of the exemplary TFM modifications is presented in Table 1.

A separate class of advancements are TFM conjunctions with other techniques such as, for example, a combining with atomic force microscopy (AFM, (Schierbaum et al., 2019)) or rheological measurements (Arevalo et al., 2011). Combining TFM with AFM is relatively straightforward as most AFMs systems are combined with optical/fluorescent microscopes. Such a system can be used for simultaneous measurements of passive viscoelastic substrates with active contractile prestress of living cells at the nanoscale (Schierbaum et al., 2019). TFM combined with rheological measurements are more demanding in terms of both sample preparation and incorporation of material viscosity into TFM calculations. On the other hand, cells sense both elastic and viscoelastic properties of the surrounding environment and use them as determinants of their functioning. In one of the experiments, a layer of collagen gels (with embedded fluorescent beads) was placed on the top of polyacrylamide hydrogels (with embedded fluorescent beads of different types). Such a sandwich was placed in the rheometer combined with fluorescent microscopy using the plane-plane geometry (Arevalo et al., 2011). The applied shear forces reorganized collagen fibres in response to applied shear stress. By analyzing their rearrangements, traction force can be quantified. A similar approach has been applied to study time-dependent changes of agarose gels functionalized with collagen. Moreover, traction forces of breast cancer cells in the interaction with such surface were quantified (Toyjanova et al., 2014b). Among advances, combining TFM with a microfluidic approach has to be underlined (Perrault et al., 2015). A comparison between static and flow conditions revealed the distinct level of traction forces generated by cells that affect our understanding of their interaction with the surrounding microenvironment in normal and pathological conditions.

4. Summary and perspectives

TFM still offers new research directions in studying traction forces at the molecular, cellular, tissue and organoid levels from its implementation in the late nineties. Thanks to TFM, the interactions between the cells and surrounding ECM and cell-cell contacts have been quantitatively elucidated. It improves our understanding of mechanisms of both the mechanical force transmission to and from cells and in the transduction of mechanical to biochemical signals and vice versa. TFM is relatively straightforward to implement; however, difficulties occur later as the techniques involve several experimental and computational approaches that are not easy. Thus, novel experimental and computational approaches are needed to be designed to enhance the TFM accuracy, especially when a 3D environment is considered. Advanced imaging and sample preparation strategies have already been reported, revealing uniques advantages and limitations as recalled here. Some exemplary directions links increased bead density and tracking accuracy with the analysis of fluorescence fluctuations (Stubb et al., 2020) or use printing technologies (Ferrari, 2019). Improvements in algorithms applied to TFs calculations are not easy as they often ask for additional biological assumptions and rarely takes into account the viscoelastic nature of bot cells and substrates. To achieve high spatial resolution, a fluctuation-based approach. Remarkable groups of advancements are linked with the combined approaches, where TFM is linked with other techniques. Further TFM requirements ask for high-throughput functionality in terms of experimental and computational time. However, various TFM-based methods are opened to novel biological and biomedical research applications with ongoing technological development.

Table 1
Summary of exemplary TFM advances used to characterize traction forces.

Name (as appeared in literature)	measured forces or stress	bead size	spacing	exemplary reference(s)
Substrate deformation				
classical 2D TFM(2D tracking)	2 – 120 nN	200 nm	~5 μm	(Dembo and Wang, 1999)
	0.05 – 0.6 kPa*	200 nm	ns	(Peschetola et al., 2013)
epifluorescent-based 3D TFM (3D tracking)	0 – 1400 Pa	200 nm	z-step size: 0.3 – 1 µm	(Hazlett et al., 2020)
quantum-dot TFM (2D & 3D tracking)	not specified 100 – 500 kPa	200 nm nanodisk	positioning: 30–45 nm images (*ab initio*) 4–8 nm	(Bergert et al., 2016)
Multidimensional TFM (2.5D tracking)	up to 500 kPa	200 nm	bead separation 1 µm	(Legant et al., 2013)
super-resolved TFM (2D tracking)	up to 0.3 kPa	40 nm	circular traction zone 1 µm	(Colin-York et al., 2016)
holographic TFM (2D tracking)	up to 10 nN	1 µm	ns	(Makarchuk et al., 2018)
traction force optical coherence microscopy (TFOCM) (3D tracking)	0 – 3 kPa 0 – 350 nN	1 µm	spacing 18 µm	(Mulligan et al., 2019)
fluctuation-based super-resolution TFM(2D tracking)	0.5 kPa – 1000 kPa	40 nm	bead density 1.2 μm^2	(Stubb et al., 2020)
Microfluidic TFM (2D tracking)				(Perrault et al., 2015)
shear stress 0.014–Pa	0 – 300 Pa	200 nm	ns	(Boldock et al., 2017) review
Tension probes				
DNA hairpin (2D tracking limited to glass surface)	4.7 pN – 2 nN 0.15–50 kPa	–	1 µm	(Morimatsu et al., 2013)
integrative tension sensor (ITS) (2D tracking, DNA-based fluorescent tension sensor)	12~54 pN	–	0.4 µm	(Wang et al., 2018)

* Depending on the stiffness of the hydrogel surface used; ns – not specified.

Declaration of Competing Interest

The authors report no declarations of interest.

Acknowledgements

ML and KG acknowledge the European Union's support under the Marie Skłodowska-Curie grant agreement No. 812772 (Phys2BioMed). AK and TZ acknowledge the support of InterDokMed project no. POWR.03.02.00-00-I013/16.

References

Arevalo, R.C., Urbach, J.S., Blair, D.L., 2011. Four-dimensional structural dynamics of sheared collagen networks. Chaos. 21, 041102.
Ariyasinghe, N.R., Reck, C.H., Viscio, A.A., Petersen, A.P., Lyra-Leite, D.M., Cho, N., McCain, M.L., 2017. Engineering micromyocardium to delineate cellular and extracellular regulation of myocardial tissue contractility. Integr. Biol. (Camb) 9, 730–741.

Bachmann, B., Spitz, S., Schädl, B., Teuschl, A.H., Redl, H., Nürnberger, S., Ertl, P., 2020. Stiffness matters: fine-tuned hydrogel elasticity alters chondrogenic redifferentiation. Front. Bioeng. Biotechnol. 8, 873.
Beningo, K.A., Dembo, M., Kaverina, I., Small, J.V., Wang, Y.L., 2001. Nascent focal adhesions are responsible for the generation of strong propulsive forces in migrating fibroblasts. J. Cell Biol. 153, 881–887.
Bergert, M., Lendenmann, T., Zündel, M., Ehret, A.E., Panozzo, D., Richner, P., Kim, D.K., Kress, S.J.P., Norris, D.J., Sorkine-Hornung, O., Mazza, E., Poulikakos, D., Ferrari, A., 2016. Confocal reference free traction force microscopy. Nat. Commun. 7, 12814.
Boldock, L., Wittkowske, C., Perrault, C.M., 2017. Microfluidic traction force microscopy to study mechanotransduction in angiogenesis. Microcirculation 24, e12361.
Brockman, J.M., Blanchard, A.T., Pui-Yan, V., Derricotte, W.D., Zhang, Y., Fay, M.E., Lam, W.A., Evangelista, F.A., Mattheyses, A.L., Salaita, K., 2018. Mapping the 3D orientation of piconewton integrin traction forces. Nat. Methods 15, 115–118.
Burdick, J.A., Chung, C., 2009. Influence of three-dimensional hyaluronic acid microenvironments on mesenchymal stem cell chondrogenesis. Tissue Eng. - Part A 15, 243–254.
Butcher, D.T., Alliston, T., Weaver, V.M., 2009. A tense situation: forcing tumour progression. Nat. Rev. Cancer 9, 108–122.
Butler, J.P., Toli-Nørrelykke, I.M., Fabry, B., Fredberg, J.J., 2002. Traction fields, moments, and strain energy that cells exert on their surroundings. Am. J. Physiol. - Cell Physiol. 282, C595–C605.
Carey, S.P., Kraning-Rush, C.M., Reinhart-King, C.A., 2011. . Single cell-mediated collagen reorganization in 3D matrices. Proceedings of the Annual International Conference of the IEEE Engineering in Medicine and Biology Society, EMBS 4333–4335.
Case, L.B., Waterman, C.M., 2015. Integration of actin dynamics and cell adhesion by a three-dimensional, mechanosensitive molecular clutch. Nat. Cell Biol. 17, 955–963.
Chang, S.S., Guo, W.H., Kim, Y., Wang, Y.L., 2013. Guidance of cell migration by substrate dimension. Biophys. J. 104, 313–321.
Colin-York, H., Shrestha, D., Felce, J.H., Waithe, D., Moeendarbary, E., Davis, S.J., Eggeling, C., Fritzsche, M., 2016. Super-resolved traction force microscopy (STFM). Nano Lett. 16, 2633–2638.
Coulombe, P.A., Lee, C.H., 2012. Defining keratin protein function in skin epithelia: epidermolysis bullosa simplex and its aftermath. J. Invest. Dermatol. 132, 763–775.
Damljanović, V., Lagerholm, B.C., Jacobson, K., 2005. Bulk and micropatterned conjugation of extracellular matrix proteins to characterized polyacrylamide substrates for cell mechanotransduction assays. Biotechniques 39, 847–851.
Del Álamo, J.C., Meili, R., Alonso-Latorre, B., Rodríguez-Rodríguez, J., Aliseda, A., Firtel, R.A., Lasheras, J.C., 2007. Spatio-temporal analysis of eukaryotic cell motility by improved force cytometry. Proc. Natl. Acad. Sci. U. S. A. 104, 13343–13348.
Delvoye, P., Wiliquet, P., Levêque, J.L., Nusgens, B.V., Lapière, C.M., 1991. Measurement of mechanical forces generated by skin fibroblasts embedded in a three-dimensional collagen gel. J. Invest. Dermatol. 97, 898–902.
Dembo, M., Wang, Y.L., 1999. Stresses at the cell-to-substrate interface during locomotion of fibroblasts. Biophys. J. 76, 2307–2316.
Doyle, A.D., Lee, J., 2002. Simultaneous, real-time imaging of intracellular calcium and cellular traction force production. Biotechniques 33, 358–364.
Elosegui-Artola, A., Oria, R., Chen, Y., Kosmalska, A., Pérez-González, C., Castro, N., Zhu, C., Trepat, X., Roca-Cusachs, P., 2016. Mechanical regulation of a molecular clutch defines force transmission and transduction in response to matrix rigidity. Nat. Cell Biol. 18, 540–548.
Ferrari, A., 2019. Recent technological advancements in traction force microscopy. Biophys. Rev. 11, 679–681.
Floor, S.L., Dumont, J.E., Maenhaut, C., Raspe, E., 2012. Hallmarks of cancer: of all cancer cells, all the time? Trends Mol. Med. 18, 509–515.
Fournier, M.F., Sauser, R., Ambrosi, D., Meister, J.J., Verkhovsky, A.B., 2010. Force transmission in migrating cells. J. Cell Biol. 188, 287–297.
Fraley, S.I., Feng, Y., Krishnamurthy, R., Kim, D.H., Celedon, A., Longmore, G.D., Wirtz, D., 2010. A distinctive role for focal adhesion proteins in three-dimensional cell motility. Nat. Cell Biol. 12, 598–604.
Fujiwara, S., Deguchi, S., Magin, T.M., 2020. Disease-associated keratin mutations reduce traction forces and compromise adhesion and collective migration. J. Cell. Sci. 133, jcs243956.
Gjorevski, N., Nelson, C.M., 2012. Mapping of mechanical strains and stresses around quiescent engineered three-dimensional epithelial tissues. Biophys. J. 103, 152–162.
Glazier, R., Brockman, J.M., Bartle, E., Mattheyses, A.L., Destaing, O., Salaita, K., 2019. DNA mechanotechnology reveals that integrin receptors apply pN forces in podosomes on fluid substrates. Nat. Commun. 10, 4507.
Grashoff, C., Hoffman, B.D., Brenner, M.D., Zhou, R., Parsons, M., Yang, M.T., McLean, M.A., Sligar, S.G., Chen, C.S., Ha, T., Schwartz, M.A., 2010. Measuring mechanical tension across vinculin reveals regulation of focal adhesion dynamics. Nature 466, 263–266.
Grinnell, F., 2000. Fibroblast-collagen-matrix contraction: growth-factor signalling and mechanical loading. Trends Cell Biol. 10, 362–365.
Grosser, S., Lippoldt, J., Oswald, L., Merkel, M., Sussman, D.M., Renner, F., Gottheil, P., Morawetz, E.W., Fuhs, T., Xie, X., Pawlizak, S., Fritsch, A.W., Wolf, B., Horn, L.-C., Briest, S., Aktas, B., Manning, M.L., Käs, J.A., 2021. Cell and nucleus shape as an Indicator of tissue fluidity in carcinoma. Phys. Rev. X 11, 011033.
Hall, M.S., Long, R., Feng, X., Huang, Y.L., Hui, C.Y., Wu, M., 2013. Toward single cell traction microscopy within 3D collagen matrices. Exp. Cell Res. 319, 2396–2408.
Hall, M.S., Alisafaei, F., Ban, E., Feng, X., Hui, C.Y., Shenoy, V.B., Wu, M., 2016. Fibrous nonlinear elasticity enables positive Mechanical feedback between cells and ECMs. Proc. Natl. Acad. Sci. U. S. A. 113, 14043–14048.
Harris, A.K., Wild, P., Stopak, D., 1980. Silicone rubber substrata: a new wrinkle in the study of cell locomotion. Science 208, 177–179.
Hazlett, L., Landauer, A.K., Patel, M., Witt, H.A., Yang, J., Reichner, J.S., Franck, C., 2020. Epifluorescence-based three-dimensional traction force microscopy. Sci. Rep. 10, 16559.
Holenstein, C.N., Silvan, U., Snedeker, J.G., 2017. High-resolution traction force microscopy on small focal adhesions-Improved accuracy through optimal marker distribution and optical flow tracking. Sci. Rep. 7, 41633.
Homberg, M., Magin, T.M., 2014. Beyond expectations: Novel insights into epidermal keratin function and regulation. Int. Rev. Cell Mol. Biol. 311, 265–306.
Hur, S.S., Zhao, Y., Li, Y.S., Botvinick, E., Chien, S., 2009. Live cells exert 3-Dimensional traction forces on their substrata. Cell. Mol. Bioeng. 2, 425–436.
Hur, S.S., Jeong, J.H., Ban, M.J., Park, J.H., Yoon, J.K., Hwang, Y., 2020. Traction force microscopy for understanding cellular mechanotransduction. BMB Rep. 53, 74–81.
Janmey, P.A., Winer, J.P., Murray, M.E., Wen, Q., 2009. The hard life of soft cells. Cell Motil. Cytoskeleton 66, 597–605.
Kai, F.B., Laklai, H., Weaver, V.M., 2016. Force matters: biomechanical regulation of cell invasion and migration in disease. Trends Cell Biol. 26, 486–497.
Kandow, C.E., Georges, P.C., Janmey, P.A., Beningo, K.A., 2007. Polyacrylamide hydrogels for cell mechanics: steps toward optimization and alternative uses. Methods Cell Biol. 83, 29–46.
Ladoux, B., Nicolas, A., 2012. Physically based principles of cell adhesion mechanosensitivity in tissues. Rep. Prog. Phys. 75, 116601.
Laflamme, M.A., Chen, K.Y., Naumova, A.V., Muskheli, V., Fugate, J.A., Dupras, S.K., Reinecke, H., Xu, C., Hassanipour, M., Police, S., O'Sullivan, C., Collins, L., Chen, Y., Minami, E., Gill, E.A., Ueno, S., Yuan, C., Gold, J., Murry, C.E., 2007. Cardiomyocytes derived from human embryonic stem cells in pro-survival factors enhance function of infarcted rat hearts. Nat. Biotechnol. 25, 1015–1024.
Le Clainche, C., Carlier, M.F., 2008. Regulation of actin assembly associated with protrusion and adhesion in cell migration. Physiol. Rev. 88, 489–513.
Lee, J., Leonard, M., Oliver, T., Ishihara, A., Jacobson, K., 1994. Traction forces generated by locomoting keratocytes. J. Cell Biol. 127, 1957–1964.
Legant, W.R., Miller, J.S., Blakely, B.L., Cohen, D.M., Genin, G.M., Chen, C.S., 2010. Measurement of mechanical tractions exerted by cells in three-dimensional matrices. Nat. Methods 7, 969–971.
Legant, W.R., Choi, C.K., Miller, J.S., Shao, L., Gao, L., Betzig, E., Chen, C.S., 2013. Multidimensional traction force microscopy reveals out-of-plane rotational moments about focal adhesions. Proc. Natl. Acad. Sci. U. S. A. 110, 881–886.
Lekka, M., 2016. Discrimination between normal and cancerous cells using AFM. Bionanoscience 6, 65–80.
Li, Z., Persson, H., Adolfsson, K., Abariute, L., Borgström, M.T., Hessman, D., Åström, K., Oredsson, S., Prinz, C.N., 2017. Cellular traction forces: a useful parameter in cancer research. Nanoscale 9, 19039–19044.
Liu, Z., Tan, J.L., Cohen, D.M., Yang, M.T., Sniadecki, N.J., Ruiz, S.A., Nelson, C.M., Chen, C.S., 2010. Mechanical tugging force regulates the size of cell-cell junctions. Proc. Natl. Acad. Sci. U. S. A. 107, 9944–9949.
Makarchuk, S., Beyer, N., Gaiddon, C., Grange, W., Hébraud, P., 2018. Holographic traction force microscopy. Sci. Rep. 8, 3038.
Mandal, K., Raz-Ben Aroush, D., Graber, Z.T., Wu, B., Park, C.Y., Fredberg, J.J., Guo, W., Baumgart, T., Janmey, P.A., 2019. Soft hyaluronic gels promote cell spreading, stress fibers, focal adhesion, and membrane tension by phosphoinositide signaling, not traction force. ACS Nano 13, 203–214.
Mark, C., Grundy, T.J., Strissel, P.L., Böhringer, D., Grummel, N., Gerum, R., Steinwachs, J., Hack, C.C., Beckmann, M.W., Eckstein, M., Strick, R., O'neill, G.M., Fabry, B., 2020. Collective forces of tumor spheroids in three-dimensional biopolymer networks. Elife 9, e51912.
Maruthamuthu, V., Sabass, B., Schwarz, U.S., Gardel, M.L., 2011. Cell-ECM traction force modulates endogenous tension at cell-cell contacts. Proc. Natl. Acad. Sci. U. S. A. 108, 4708–4713.
McCain, M.L., Lee, H., Aratyn-Schaus, Y., Kléber, A.G., Parker, K.K., 2012. Cooperative coupling of cell-matrix and cell-cell adhesions in cardiac muscle. Proc. Natl. Acad. Sci. U. S. A. 109, 9881–9886.
McCain, M.L., Yuan, H., Pasqualini, F.S., Campbell, P.H., Parker, K.K., 2014. Matrix elasticity regulates the optimal cardiac myocyte shape for contractility. Am. J. Physiol. - Hear. Circ. Physiol. 306, H1525–H1539.
McKenzie, A.J., Hicks, S.R., Svec, K.V., Naughton, H., Edmunds, Z.L., Howe, A.K., 2018. The mechanical microenvironment regulates ovarian cancer cell morphology, migration, and spheroid disaggregation. Sci. Rep. 8, 7228.
Medina, S.H., Bush, B., Cam, M., Sevcik, E., DelRio, F.W., Nandy, K., Schneider, J.P., 2019. Identification of a mechanogenetic link between substrate stiffness and chemotherapeutic response in breast cancer. Biomaterials 202, 1–11.
Meng, F., Suchyna, T.M., Sachs, F., 2008. A fluorescence energy transfer-based mechanical stress sensor for specific proteins in situ. FEBS J. 275, 3072–3087.
Mertz, A.F., Che, Y., Banerjee, S., Goldstein, J.M., Rosowski, K.A., Revilla, S.F., Niessen, C.M., Marchetti, M.C., Dufresne, E.R., Horsley, V., 2013. Cadherin-based intercellular adhesions organize epithelial cell-matrix traction forces. Proc. Natl. Acad. Sci. U. S. A. 110, 842–847.
Messi, Z., Bornert, A., Raynaud, F., Verkhovsky, A.B., 2020. Traction forces control cell-edge dynamics and mediate distance sensitivity during cell polarization. Curr. Biol. 30, 1762-1769.e5.
Meyer, A.S., Hughes-Alford, S.K., Kay, J.E., Castillo, A., Wells, A., Gertler, F.B., Lauffenburger, D.A., 2012. 2D protrusion but not motility predicts growth factor-induced cancer cell migration in 3D collagen. J. Cell Biol. 197, 721–729.
Morimatsu, M., Mekhdjian, A.H., Adhikari, A.S., Dunn, A.R., 2013. Molecular tension sensors report forces generated by single integrin molecules in living cells. Nano Lett. 13, 3985–3989.
Mulligan, J.A., Feng, X., Adie, S.G., 2019. Quantitative reconstruction of time-varying 3D cell forces with traction force optical coherence microscopy. Sci. Rep. 9, 4086.

Murray, J.D., Oster, G.F., 1984. Cell traction models for generating pattern and form in morphogenesis. J. Math. Biol. 19, 265–279.
Oakes, P.W., Banerjee, S., Marchetti, M.C., Gardel, M.L., 2014. Geometry regulates traction stresses in adherent cells. Biophys. J. 107, 825–833.
Oliver, T., Jacobson, K., Dembo, M., 1995. Traction forces in locomoting cells. Cell Motil. Cytoskeleton 31, 225–240.
Orzechowska, B., Pabijan, J., Wiltowska-Zuber, J., Zemła, J., Lekka, M., 2018. Fibroblasts change spreading capability and mechanical properties in a direct interaction with keratinocytes in conditions mimicking wound healing. J. Biomech. 74, 134–142.
Park, J.S., Burckhardt, C.J., Lazcano, R., Solis, L.M., Isogai, T., Li, L., Chen, C.S., Gao, B., Minna, J.D., Bachoo, R., DeBerardinis, R.J., Danuser, G., 2020. Mechanical regulation of glycolysis via cytoskeleton architecture. Nature 578, 621–626.
Pasqualini, F.S., Agarwal, A., O'Connor, B.B., Liu, Q., Sheehy, S.P., Parker, K.K., 2018. Traction force microscopy of engineered cardiac tissues. PLoS One 13, e0194706.
Pelham, R.J., Wang, Y.L., 1997. Cell locomotion and focal adhesions are regulated by substrate flexibility. Proc. Natl. Acad. Sci. U. S. A. 94, 13661–13665.
Perrault, C.M., Brugues, A., Bazellieres, E., Ricco, P., Lacroix, D., Trepat, X., 2015. Traction forces of endothelial cells under slow shear flow. Biophys. J. 109, 1533–1536.
Peschetola, V., Laurent, V.M., Duperray, A., Michel, R., Ambrosi, D., Preziosi, L., Verdier, C., 2013. Time-dependent traction force microscopy for cancer cells as a measure of invasiveness. Cytoskeleton 70, 201–214.
Pogoda, K., Bucki, R., Byfield, F.J., Cruz, K., Lee, T., Marcinkiewicz, C., Janmey, P.A., 2017. Soft substrates containing hyaluronan mimic the effects of increased stiffness on morphology, motility, and proliferation of glioma cells. Biomacromolecules 18, 3040–3051.
Polacheck, W.J., Chen, C.S., 2016. Measuring cell-generated forces: A guide to the available tools. Nat. Methods 13, 415–423.
Rape, A., Guo, W.H., Wang, Y.L., 2011. Microtubule depolymerization induces traction force increase through two distinct pathways. J. Cell. Sci. 124, 4233–4240.
Razafiarison, T., Holenstein, C.N., Stauber, T., Jovic, M., Vertudes, E., Loparic, M., Kawecki, M., Bernard, L., Silvan, U., Snedeker, J.G., 2018. Biomaterial surface energy-driven ligand assembly strongly regulates stem cell mechanosensitivity and fate on very soft substrates. Proc. Natl. Acad. Sci. U. S. A. 115, 4631–4636.
Reinhart-King, C.A., Dembo, M., Hammer, D.A., 2008. Cell-cell mechanical communication through compliant substrates. Biophys. J. 95, 6044–6051.
Roca-Cusachs, P., Conte, V., Trepat, X., 2017. Quantifying forces in cell biology. Nat. Cell Biol. 19, 742–751.
Schierbaum, N., Rheinlaender, J., Schäffer, T.E., 2019. Combined atomic force microscopy (AFM) and traction force microscopy (TFM) reveals a correlation between viscoelastic material properties and contractile prestress of living cells. Soft Matter 15, 1721–1729.
Schwarz, U.S., Balaban, N.Q., Riveline, D., Bershadsky, A., Geiger, B., Safran, S.A., 2002. Calculation of forces at focal adhesions from elastic substrate data: the effect of localized force and the need for regularization. Biophys. J. 83, 1380–1394.
Schwarz, U.S., Balaban, N.Q., Riveline, D., Addadi, L., Bershadsky, A., Safran, S.A., Geiger, B., 2003. Measurement of cellular forces at local adhesion using elastic micro- patterned substrates. Mater. Sci. Eng. C 23, 387–394.
Scotton, C.J., Wilson, J.L., Milliken, D., Balkwill, F.R., Stamp, G., 2001. Epithelial cancer cell migration: A role for chemokine receptors? Cancer Res. 61, 4961–4965.
Steinwachs, J., Metzner, C., Skodzek, K., Lang, N., Thievessen, I., Mark, C., Münster, S., Aifantis, K.E., Fabry, B., 2016. Three-dimensional force microscopy of cells in biopolymer networks. Nat. Methods 13, 171–176.
Stubb, A., Laine, R.F., Miihkinen, M., Hamidi, H., Guzmán, C., Henriques, R., Jacquemet, G., Ivaska, J., 2020. Fluctuation-based super-resolution traction force microscopy. Nano Lett. 20, 2230–2245.
Style, R.W., Boltyanskiy, R., German, G.K., Hyland, C., Macminn, C.W., Mertz, A.F., Wilen, L.A., Xu, Y., Dufresne, E.R., 2014. Traction force microscopy in physics and biology. Soft Matter 10, 4047–4055.
Sunyer, R., Jin, A.J., Nossal, R., Sackett, D.L., 2012. Fabrication of hydrogels with steep stiffness gradients for studying cell mechanical response. PLoS One 7, e46107.
Sunyer, R., Conte, V., Escribano, J., Elosegui-Artola, A., Labernadie, A., Valon, L., Navajas, D., García-Aznar, J.M., Muñoz, J.J., Roca-Cusachs, P., Trepat, X., 2016. Collective cell durotaxis emerges from long-range intercellular force transmission. Science 353, 1157–1161.
Svitkina, T., 2018. The actin cytoskeleton and actin-based motility. Cold Spring Harb. Perspect. Biol. 10, a018267.
Szabó, A., Mayor, R., 2015. Cell traction in collective cell migration and morphogenesis: the chase and run mechanism. Cell Adhes. Migr. 9, 380–383.
Tang, X., Kuhlenschmidt, T.B., Zhou, J., Bell, P., Wang, F., Kuhlenschmidt, M.S., Saif, T. A., 2010. Mechanical force affects expression of an in vitro metastasis-like phenotype in HCT-8 cells. Biophys. J. 99, 2460–2469.
Tang, X., Bajaj, P., Bashir, R., Saif, T.A., 2011. How far cardiac cells can see each other mechanically. Soft Matter 7, 6151–6158.
Tang, X., Yakut Ali, M., Saif, M.T.A., 2012. A novel technique for micro-patterning proteins and cells on polyacrylamide gels. Soft Matter 8, 7197–7206.
Tang, X., Tofangchi, A., Anand, S.V., Saif, T.A., 2014. A novel cell traction force microscopy to study multi-cellular system. PLoS Comput. Biol. 10, e1003631.
Toyjanova, J., Bar-Kochba, E., López-Fagundo, C., Reichner, J., Hoffman-Kim, D., Franck, C., 2014a. High resolution, large deformation 3D traction force microscopy. PLoS One.
Toyjanova, J., Hannen, E., Bar-Kochba, E., Darling, E.M., Henann, D.L., Franck, C., 2014b. 3D Viscoelastic traction force microscopy. Soft Matter 10, 8095–8106.
Trepat, X., Wasserman, M.R., Angelini, T.E., Millet, E., Weitz, D.A., Butler, J.P., Fredberg, J.J., 2009. Physical forces during collective cell migration. Nat. Phys. 5, 426–430.
Vining, K.H., Mooney, D.J., 2017. Mechanical forces direct stem cell behaviour in development and regeneration. Nat. Rev. Mol. Cell Biol. 18, 728–742.
Wang, N., 2017. Review of cellular mechanotransduction. J. Phys. D Appl. Phys. 50, 233002.
Wang, J.H.C., Lin, J.S., 2007. Cell traction force and measurement methods. Biomech. Model. Mechanobiol. 6, 361–371.
Wang, S., Wolynes, P.G., 2012. Active contractility in actomyosin networks. Proc. Natl. Acad. Sci. U. S. A. 109, 6446–6451.
Wang, H.B., Dembo, M., Wang, Y.L., 2000. Substrate flexibility regulates growth and apoptosis of normal but not transformed cells. Am. J. Physiol. - Cell Physiol. 279, C1345–C1350.
Wang, Y., LeVine, D.N., Gannon, M., Zhao, Y., Sarkar, A., Hoch, B., Wang, X., 2018. Force-activatable biosensor enables single platelet force mapping directly by fluorescence imaging. Biosens. Bioelectron. 100, 192–200.
Wheelwright, M., Win, Z., Mikkila, J.L., Amen, K.Y., Alford, P.W., Metzger, J.M., 2018. Investigation of human iPSC-derived cardiac myocyte functional maturation by single cell traction force microscopy. PLoS One 13, e0194909.
Yang, Z., Lin, J.S., Chen, J., Wang, J.H.C., 2006. Determining substrate displacement and cell traction fields-a new approach. J. Theor. Biol. 242, 607–616.
Zemła, J., Bobrowska, J., Kubiak, A., Zieliński, T., Pabijan, J., Pogoda, K., Bobrowski, P., Lekka, M., 2020. Indenting soft samples (hydrogels and cells) with cantilevers possessing various shapes of probing tip. Eur. Biophys. J. 49, 485–495.